

# Magnetic properties of $\alpha$ -iron (II) phthalocyanine

M. Evangelisti

Kamerlingh Onnes Laboratory, Leiden University, 2300 RA, Leiden, The Netherlands, and  
Instituto de Ciencia de Materiales de Aragon, C.S.I.C. – Universidad de Zaragoza, 50009 Zaragoza, Spain

J. Bartolomé

Instituto de Ciencia de Materiales de Aragon, C.S.I.C. – Universidad de Zaragoza, 50009 Zaragoza, Spain

L. J. de Jongh

Kamerlingh Onnes Laboratory, Leiden University, 2300 RA, Leiden, The Netherlands

G. Filoti

National Institute for Materials Physics, P.O. Box MG-07, 76900 Bucharest-Magurele, Romania  
(Dated: April 14, 2024)

We report on the magnetic properties of the supra-molecular compound iron (II) phthalocyanine in its  $\alpha$ -form. dc- and ac-susceptometry measurements and Mössbauer experiments show that the iron atoms are strongly magnetically coupled into ferromagnetic Ising chains with very weak antiferromagnetic interchain coupling. The transition to 3D magnetic ordering below 10 K is hindered by the presence of impurities or other defects, by which the domain-wall arrangements along individual chains become gradually blocked/frozen, leading to a disordered 3D distribution of ferromagnetic chain segments. Below 5 K, field-cooled and zero-field-cooled magnetization measurements show strong irreversible behavior, attributed to pinning of the domain-walls by the randomly distributed defects in combination with the interchain coupling. High-field magnetization experiments reveal a canted arrangement of the moments in adjacent ferromagnetic chains.

PACS numbers: 75.50.Xx; 76.80.+y

## I. INTRODUCTION

Metal phthalocyanines (hereafter referred to as MPC) have received extensive attention in the last three decades because of their commercial applications as dyes, catalysts, and because of their interesting electro-optical properties [1, 2]. Their magnetic properties have attracted attention as well since manganese phthalocyanine (MnPC) was one of the first molecular magnets [3]. In this work we focus on iron (II) phthalocyanine (FePC).

In the MPC molecule, the M atom has square planar coordination with four pyrrolic N atoms. In the bulk and in thin films, these planar molecules form linear chains by columnar stacking. The molecules are tilted by an angle with respect to the chain axis [4, 5]. The angle at the parallel adjacent chain is opposite, thus constructing a so-called "herringbone" structure. The different angles and relative positions of the chains give rise to different polymorphs, for example in the  $\alpha$  and  $\beta$  forms of copper phthalocyanine (CuPC) [5]. This is of importance since the magnetic properties of metal complexes are strongly dependent on structural differences. For example, the particular structure in the  $\beta$ -MnPC is thought to underly the Mn(Mn) ferromagnetic interactions that make this compound the only ferromagnetic MPC compound so far reported [3].

A very similar molecule with square planar M coordination is M-porphyrine. These molecules may also stack in different polytypes, giving rise to different magnetic properties. Very recently it was reported that Fe(II) oc-

taethyltetraazaporphyrin crystallizes in two structures: the  $\alpha$ -form which is a canted, soft molecular ferromagnet with  $T_c = 5.6$  K, and the  $\beta$ -form which remains paramagnetic down to 1 K [6, 7]. Apparently, though the Fe(II) electronic states are identical, the different exchange paths and distances between the neighboring molecules and between chains modulate the magnetic behavior. Thus, also Fe(II) square coordinated complexes seem prone to show various types of magnetic behavior.

FePC could fall into this category of magnetic complexes. There are two forms of FePC described in the literature. The  $\alpha$ -form is metastable and obtained either as a polycrystalline powder or as a thin film formed by vacuum deposition onto a cold substrate [8, 9]. The  $\beta$ -form is the most stable one and is obtained not only from the sublimation technique in the form of a single crystal, but also from heating the  $\alpha$ -form sample to 350 °C for a few hours [8]. Since 1935, the  $\beta$ -form of this compound has been repeatedly reported to behave as a singlet-ground-state paramagnet down to the lowest measured temperatures [4, 10, 11, 12]. On the other hand, to the best of our knowledge, the magnetic properties of  $\alpha$ -FePC have so far never been studied. We show below that in the  $\alpha$ -form of FePC the Fe(II) moments are strongly coupled into ferromagnetic chains, with the weak interchain coupling leading to a canted, soft molecular ferromagnet below about 10 K. Our findings demonstrate that FePC has a behavior very similar to MnPC, so the magnetic behavior of the latter is not so exotic as thought earlier [3], but is a member of a more general category of square-planar

metal complexes in which ferromagnetic correlations are established. They represent, therefore, quite interesting examples of molecular magnets, a subject of intensive on-going research [13].

## II. EXPERIMENTAL DETAILS

All the experiments were performed on powdered samples of the  $\beta$ -FePc compound as obtained from Aldrich company (catalogue number 37,954.9), in two different batches. We verified the stoichiometry by elemental analysis. The morphology was studied by scanning electron microscopy with a resolution of 3.5 nm. A step scanned powder X-ray diffraction pattern was collected at room temperature using a rotating anode X-ray diffractometer. The diffractometer was operated at 80 mA and 40 kV with Cu radiation and a graphite monochromator was used to select the  $\text{Cu K}_{1/2}$  radiation. Data were collected from  $4^\circ$  up to  $90^\circ$  with a step size of  $0.02^\circ$  and a counting rate of 4 s/step.

Magnetic data were obtained with the use of a commercial SQUID based ac-magnetometer instrument down to 1.7 K with an external magnetic field in the range 50 to 50 kOe. The amplitude of the ac-field was 4.5 Oe in all the experiments and the frequency  $f$  was varied between 0.1 and 1380 Hz. Magnetic data with larger applied field (up to 200 kOe) were obtained in the Nijmegen High Field Magnet Laboratory. The magnetization was measured using the ballistic extraction technique and the sensitivity was about  $10^{-3}$  emu. The heat capacity was measured from 1.8 K up to 20 K with a commercial calorimeter.

## III. MORPHOLOGY AND STRUCTURE

By scanning electron microscopy, we have observed that  $\beta$ -FePc develops in crystallites whose shape is similar to a 'bunch of rods' (Fig. 1). The ratio of length to thickness is approximately 10. Without any preferred length, the crystallites can be as long as up to hundreds of micrometers. By means of powder X-ray diffraction we have found that the present form of  $\beta$ -FePc is isomorphic to the  $\beta$ -form of 4-monochloro-copper phthalocyanine [5], that is triclinic with space group  $P1$  or  $P\bar{1}$ . The  $\theta$  of the X-ray diffraction spectrum provides the following cell dimensions:  $a = 12.2 \text{ \AA}$ ,  $b = 3.78 \text{ \AA}$ ,  $c = 13.0 \text{ \AA}$ ,  $\alpha = 90.0^\circ$ ,  $\beta = 90.4^\circ$  and  $\gamma = 95.6^\circ$ . The  $\theta$  to the peak intensities is not good due to the needle shape of the powder grains that produces a texture effect. Thus, in the present sample of  $\beta$ -FePc the molecules are stacked parallel to each other along the short  $b$ -axis at intervals of  $3.78 \text{ \AA}$ , and the molecular planes are inclined to the  $ac$  plane at an angle of  $26.5^\circ$ , in a herringbone structure (Fig. 2). The vertical distance between the neighboring molecules is about  $3.4 \text{ \AA}$ . We have verified further that the present form of  $\beta$ -FePc is indeed the (metastable)  $\beta$ -form because it shows

the characteristic IR-absorption peak at  $250 \text{ cm}^{-1}$  [9]. By warming our sample at  $350^\circ \text{C}$  during 24 hours in vacuum, the compound transforms into the  $\alpha$ -form, as expected.

In the  $\beta$ -form, the Fe atom is coordinated to the four N atoms in the diagonal positions of the square planar molecule. The nearest neighbors on the adjacent molecule at one side are the two isoindole and one azamethine nitrogens located at similar distances, while at the other side the coordination is identical but rotated by  $180^\circ$ . The Fe(II) ion is in a symmetry lower than  $D_{4h}$ , but in a first approximation we shall assume this local symmetry. The value of  $3.78 \text{ \AA}$  for the Fe-Fe separation along the  $b$ -axis in the present form of  $\beta$ -FePc is very reasonable, lying within the accepted range of  $3.5\text{--}4.8 \text{ \AA}$  for metalloporphyrin dimers [14]. It is generally accepted that the Fe-Fe separation along the  $b$ -axis and the angle of inclination of the molecular planes with respect to the crystallographic  $ac$  plane determine the extent of the exchange Fe-Fe interaction.

We note that the main structural difference with the  $\alpha$ -form consists in the inclination angle (Fig. 2); in the  $\alpha$ -form it is  $45.8^\circ$  and the azamethine nitrogen of each adjacent molecule lays just on the apical position of an octahedron of N atoms [5], in the  $\beta$ -form it is  $26.5^\circ$ , and the N atoms from the nearest molecules are not in axial positions and therefore do not form such a N octahedron about the Fe atom.

## IV. EXPERIMENTAL RESULTS

The inverse of the in-phase component of the zero-field ac-susceptibility of  $\beta$ -FePc, as measured at  $f = 90 \text{ Hz}$ , is plotted as a function of temperature in Fig. 3. As shown by the solid line, the data can be fitted between 50 K and 300 K by a Curie-Weiss law  $\chi^{-1} = C/(T - \theta)$  for  $S = 1$ ,  $g = 2.54$  and  $\theta = (40 \pm 2) \text{ K}$ . This result implies that in this temperature range the iron (II) ion is in an effective spin  $S = 1$  state, and the large positive value of  $\theta$  indicates that there are strong ferromagnetic correlations between the Fe moments in the paramagnetic phase. On basis of the powder X-ray structural analysis, we expect these correlations to extend within the columnar chains along the  $b$ -axis. Neglecting interchain magnetic coupling and using the mean-field expression for the Curie-Weiss temperature  $\theta = 2zJS(S+1)/3k_B$ , we find for  $S = 1$  and  $z = 2$  the estimate  $J = k_B \theta / 15 \text{ K}$  for the ferromagnetic interaction strength along the chains. We note that also for the  $\alpha$ -form of  $\beta$ -FePc, an effective spin  $S = 1$  was found below room temperature. Indeed, at high temperatures, the susceptibilities of the  $\alpha$  and  $\beta$  [4, 15] forms are coincident (inset of Fig. 3). The fact that the susceptibility of the  $\beta$ -form goes to zero for  $T \rightarrow 0$  has been explained in terms of zero-field splitting of the triplet state, leaving a non-magnetic singlet as the lowest energy level occupied for  $T \rightarrow 0 \text{ K}$  [4].

Turning now to the data taken below 50 K, as exempli-

ed in Fig. 4, we note that the behavior of the susceptibility of  $\text{FePc}$  points to strong low-dimensional magnetic characteristics [16]. Indeed, as seen in Fig. 4, the susceptibility continues to increase down to temperatures much lower than  $T_C$ . Only at about 10 K the ac-susceptibility curve shows a change of slope, and a rounded maximum is found at still lower temperatures. The paramagnetic behavior is thus sustained down to approximately 10 K, that is much less than  $T_C$ , as expected for a magnetic chain system [16].

From the shape of the  $\chi''(T)$  curve in Fig. 4, one would be tempted to associate the change of slope to the onset of 3D correlations between the chains due to antiferromagnetic interchain coupling. However, here we should point to the fact that  $\chi''$  at the maximum is not very far below the calculated limit for a completely ferromagnetically ordered isotropic material below  $T_C$ , namely  $1/N$  with  $N$  the demagnetizing factor (a rough estimate gives the value of  $33 \text{ emu/mol}$ ).

Since the presence of anisotropy can lower the value of the susceptibility of a ferromagnetic powder considerably [16, 17], the occurrence of ferromagnetic interchain ordering would also be considered. Moreover, in case the moments of the ferromagnetic chains would be subject to strong crystal field anisotropy, the latter could compete with the interchain interactions, and, when sufficiently strong, lead to a freezing at some blocking temperature before the interchain coupling becomes effective (analogous to the phenomena observed in molecular magnetic clusters and superparamagnetic particles).

In order to further investigate the nature of the "ordering" processes, we have therefore measured the zero-field differential susceptibility in the region below 15 K for different frequencies. The dependence on frequency of the real and imaginary parts of the ac-susceptibility are shown in Fig. 5. As was already seen for  $f = 90 \text{ Hz}$  in Fig. 4, for all frequencies used the in-phase component of the ac-susceptibility,  $\chi'$ , shows a rounded maximum in the range 5 K {10 K. This is always accompanied by a maximum in the out-of-phase component,  $\chi''$ , at somewhat lower temperature. The maximum in  $\chi''(T)$  shifts to lower temperature with decreasing frequency, and  $\chi''(T)$  decreases abruptly to zero below the maximum. The sharp maximum in  $\chi''(T)$  shifts likewise with frequency. It is not possible then to define a definite transition temperature to a 3D ordered state from these data, since the obtained  $T_C$  would be frequency dependent. The shift in temperature of the maximum in  $\chi''(T)$  and  $\chi''(T)$  with the frequency are reminiscent of spin-glass or superparamagnetic behavior. Since the freezing temperature  $T_f(!)$  can be defined from  $! [T_f(!); H = 0] = 1$ , a quantitative measure of the frequency shift is obtained from  $(T_f(!) - T_f(!)) = \ln(!) = 0.034$ . It is six times larger than the rate for a metallic spin glass and an order of magnitude smaller than for a superparamagnet [18].

In view of the just-described frequency dependence of the ac-susceptibility, we decided to investigate the analogy with spin glass systems or superparamagnets still

further, by means of dc-magnetization studies. In Fig. 6 we show dc- $M(T)$  measurements taken with the SQUID magnetometer in the zero-field cooling (ZFC) and ed-cooling (FC) modes at two fields,  $H = 50 \text{ Oe}$  and  $1 \text{ kOe}$ . We note that both curves show a change in slope at about 10 K, similar as for  $\chi''$  in Figs. 4 and 5. Furthermore, a bifurcation point showing strong irreversibility is found below about 5 K. At first sight, the bifurcation temperature is not much affected by the field although we point out that for the low-field curve (50 Oe) the ZFC and FC curves strictly speaking only coincide above  $T \approx 10 \text{ K}$ .

In another experiment, after a FC process down to 1.8 K with  $H = 40 \text{ Oe}$  the field was switched on and the remnant magnetization was measured (Fig. 7). We found a large remnant magnetization at 1.8 K which very rapidly decays by several orders of magnitude when increasing the temperature towards 5 K. Above 5 K, the decay of the remanence proceeds much slower (inset of Fig. 7), and a small amount of remnant magnetization is seen to persist even up to 10 K {15 K. On basis of Fig. 7 we may conclude that, although most of the field-induced magnetization is indeed lost at about 5 K, a small fraction of about 3% is left above this temperature, and is only removed by warming up to about 15 K. This behavior points to the presence of substantial ferromagnetic short-range order along the chains in this intermediate region of 5 K {15 K, in agreement with the behavior of the ac-susceptibility.

The  $M(H)$  measurements of the initial (ZFC) magnetization were therefore extended to higher fields and at temperatures above, at and below this intermediate region in order to get some more insight in these irreversibility processes (Fig. 8). The data at  $T = 30 \text{ K}$  show the expected paramagnetic behavior. In the intermediate temperature region, for  $T = 8 \text{ K}$  and  $5 \text{ K}$ , the initial increase in  $M(H)$  is very abrupt, reaching the value  $1.4 \mu_B$  for  $H = 2.5 \text{ kOe}$ . Above 10 kOe, the magnetization curves measured with the SQUID up to 50 kOe (Fig. 8) or in the Nijmegen High Field Magnet Laboratory (Fig. 9), show an additional slow increase up to  $\mu_B$  at  $H = 200 \text{ kOe}$ . Note in Fig. 9 the perfect coincidence of the SQUID equilibrium measurement with the branch corresponding to the high-field measurement at decreasing field, while the branch measured at increasing field is lower. The SQUID measurements have a characteristic point-to-point measuring time of 150 s while the high-field measurements have a characteristic time of 40 s. The system evidently needs a longer time than 40 s to reach equilibrium at this temperature when the field is increased from zero.

The spontaneous magnetization evaluated as the extrapolation to  $H = 0$  of the high field demagnetizing curve yields a value of  $1.5 \mu_B$ . We point out that, although these measurements demonstrate that in the region below about 5 K the compound is in a ferromagnetic state, when the g factor deduced in the paramagnetic region is still valid in this range, the saturation magnetization would be  $2.5 \mu_B$  on basis of the (effective) spin

$S = 1$  ground state found for the Fe(II) ions from the Curie-Weiss analysis of the high-temperature susceptibility (Fig. 3). We shall come back to this discrepancy below in the discussion section, where we shall argue that on basis of the competition between the exchange term and the crystal field term in the Hamiltonian for  $\text{FePc}$ , a substantial canting of the magnetic moments with respect to the crystal field (anisotropy) axis is to be expected. The increases seen in the  $M(H)$  curves above 5 kOe may then be associated with the gradual rotation of the canted moments, produced by the competition between the Zeeman energy and the crystal field energy.

One may conclude that below 5 K, the material shows strong irreversibility, as already evidenced by the bifurcation point in Fig. 6. Also the behavior of the  $M(H)$  curves in Fig. 8 points to the presence of long relaxation times. For example, the initial  $M(H)$  curve measured at 1.8 K is actually even lower than the data at 15 K, since the time waited to measure each point is of the order of minutes and only a fraction of the sample is oriented. This is more clearly seen in the hysteresis loop measured at 1.8 K by sweeping the field between -50 and 50 kOe in a time of 150 s (Fig. 10). The initial curve increases progressively with the field, tending to a value of  $1.6 \mu_B$  at 20 kOe. When the field decreases, the magnetization remains nearly constant down to zero-field, yielding a remanence of  $1.5 \mu_B$ . However, the inversion of the remanent moment is very abrupt when a field in the opposite direction is applied, indicating that there is no coercivity in the usual sense associated with this remanence.

Similarly strong relaxation effects in the low-temperature range have been seen in preliminary  $^{57}\text{Fe}$  Mossbauer spectroscopic studies on  $\text{FePc}$ . In Fig. 11 spectra at some representative temperatures are shown. Above 25 K, the spectrum is hardly temperature dependent and reveals the familiar paramagnetic, quadrupolar split doublet. Below that temperature the doublet starts gradually to broaden and below about 15 K a magnetic hyperfine splitting appears, at first extremely broadened, then becoming the sharper the lower the temperature. Below about 5 K, the broadening has almost disappeared and a fully hyperfine split spectrum is observed. A detailed presentation of the Mossbauer spectra will be given in another publication.

Similar temperature dependent relaxation phenomena as seen in the Mossbauer spectra in Fig. 11, have typically been seen for blocking phenomena in superparamagnetic particles or for domain-wall excitations in anisotropic magnetic (Ising) chains. Briefly, the magnetic moment of the Mossbauer nucleus (here  $^{57}\text{Fe}$ ) feels the hyperfine field exerted on it by the electron spin on the same atom. Thus the fluctuations in the hyperfine field are directly related to the electron spin dynamics, i.e. the nuclear moment probes the autocorrelation function of the electron spin. Accordingly, the Mossbauer spectrum will be broadened as long as the fluctuation rate of the electron spin lies in the frequency window ( $10^6$  Hz to  $10^9$  Hz) of the Mossbauer experiment. The temperature dependence

observed indicates that the electron spin dynamics is described by thermally activated processes. At high temperatures the fluctuation rate of the electron spins is too fast to cause broadening. With lowering temperature the rate slows down, enters the Mossbauer frequency window leading to the strong relaxation. At the lower temperatures the rate becomes just too slow to be felt. In superparamagnetic particles, the activated process is related to the thermally excited switching of the particle's magnetic moment between the orientations dictated by the anisotropy, which becomes blocked at low temperatures. In the magnetic Ising chain systems, the fluctuation rate is dictated by the density of thermally excited domain-walls (solitons) along the chains. At high temperatures, the density is very high and thus the fluctuations too fast. At intermediate temperatures, the fluctuation rate passes the Mossbauer window, whereas, at low temperatures, the soliton density becomes too small, moreover the walls may become blocked/pinned by interchain interactions or defects in the chains.

## V. DISCUSSION

Summing up the evidence obtained so far, we may state that the magnetic structure of  $\text{FePc}$  is most probably composed of very weakly coupled ferromagnetic chains, with an intrachain exchange  $J = k_B \cdot 15$  K, and an effective spin  $S = 1$  for the Fe(II) ion in the temperature range 50 K to 300 K. The crystal field splitting, responsible for the effective spin  $S = 1$ , likely result in addition into a strong anisotropy of the ferromagnetic interaction. Below, we shall thus start the discussion with a full analysis of the crystal field effects in this material, in particular also in relation to the other members of the metal phthalocyanine and metal porphyrine family. Next we shall present the ensuing analysis of the magnetic susceptibility in the range 10 K to 50 K in terms of 1D magnetic models systems. Finally, the nature of the relaxation and ordering phenomena observed below 15 K will be further analyzed.

As is well known, for Fe(II) the combination of orthorhombic crystal field splitting combined with spin-orbit coupling leads to an effective spin description for the five lowest occupied levels ( $d_{xy}; d_{yz}; d_{xz}; d_{z^2}; d_{x^2-y^2}$ ) [19, 20]. Depending on the ratio of the parameters, and the relevant temperatures of the experiment, one can have a situation where either two, three or all five levels will participate in the magnetic ordering processes, leading to an effective spin  $S = 1/2, 1$  or  $2$ , respectively, for the Fe(II) ion. For thermal energies in the range 100 K to 300 K, the  $\text{FePc}$  may be described as an effective spin  $S = 1$  with  $g = 2.54$ . However, the thermally occupied levels, which lead to the  $S = 1$ , are split into a lower-lying singlet and an excited doublet, with the splitting being probably of the order of 50 K. Accordingly, the magnetic behavior will be determined by the competition between the magnetic exchange energy and the crystal field term rep-

representing this singlet-doublet splitting. From the Curie-Weiss law to the susceptibility, we have seen that  $\sim 40$  K, so both these terms are of the same order of magnitude. Below we will show that the competition may actually produce a canted arrangement of the ferromagnetically aligned spins, with an effective spin  $S = 1/2$  at low temperatures and considerable anisotropy.

For the temperature range 100 K–300 K, we conclude that the Fe(II) ion in  $\text{FePc}$  may be described as an effective spin  $S = 1$  compound, in which single-ion anisotropy and second-order spin-orbit coupling leaves the triplet as the lowest energy multiplet. This is the same spin state as found in  $\text{MnPc}$  [4]. Indeed, both compounds have identical magnetic properties at room temperature, which arise from a similarly split triplet [ $D = k_B \cdot 53$  K and 98 K, for  $\text{MnPc}$  and  $\text{FePc}$ , respectively (see below)] with the non-magnetic singlet as the ground state [15].

In the  $\text{MnPc}$  form the  $S = 1$  spins remain ferromagnetically coupled in magnetic chains down to the lowest temperatures in spite of the non-magnetic ground singlet since the ferromagnetic interaction  $2zJ$  (with  $J = k_B \cdot 15$  K as estimated from the Curie-Weiss law) is larger than  $D$ , in agreement with Moriya's criterion for magnetic ordering in a  $S = 1$  triplet [21]. Apparently, this condition is not satisfied in  $\text{FePc}$  because the ratio of  $D$  over  $J$  is larger, and as a consequence it remains paramagnetic at all temperatures.

Curiously, the magnetic phenomenology of the  $\text{MnPc}$  forms is just opposite: i.e. the  $\text{MnPc}$  form is ferromagnetic while the  $\text{FePc}$  form is antiferromagnetic [22]. In the  $\text{MnPc}$  compounds the different behavior of the two forms was attributed to competing ferro- and antiferromagnetic exchange interactions, neglecting direct Mn-Mn coupling. Under the assumption that the electronic configuration of the  $3d^5$  electrons is  $(d_{xy})^2 (d_{xz})^1 (d_{yz})^1 (d_{z^2})^1$ , the ferromagnetic interaction is caused by the overlap between the  $d_{z^2}$  unpaired electron ( $a_{1g}$  symmetry) with the  $d_{xy}$  orbital of  $E_g$  symmetry of the adjacent aromatic ring, which is orthogonal to the  $d_{z^2}$  orbital of its metal ion (Fig. 12). The antiferromagnetic coupling is due to the overlap of the  $d_{xz}d_{yz}$  orbitals ( $e_g$ ) with the same  $d_{xy}$  orbital of  $E_g$  symmetry (Fig. 12). In the  $\text{MnPc}$  form the ferromagnetic mechanism dominates while in the  $\text{FePc}$  form the ferromagnetic path weakens and antiferromagnetism prevails [22].

If we assume that the electronic configuration of Fe is related to that of the Mn by just adding one electron to the second level as proposed for the  $\text{FePc}$  form by Dale et al. [12] and Coops et al. [23], that is  $E_g A_1 (d_{xy})^2 (d_{xz})^2 (d_{yz})^1 (d_{z^2})^1$ , then the same arguments as for the Mn compounds would be applicable. The only difference would be that the antiferromagnetic interaction should be weakened, since the  $(d_{xz}; d_{yz})$  doublet should have just one unpaired electron. Consequently, the  $\text{FePc}$  form should be ferromagnetic, contrary to observation. One arrives to the same conclusion if one assumes the electronic configuration  $B_{2g} (d_{xy})^1 (d_{xz})^2 (d_{yz})^2 (d_{z^2})^1$ , as

proposed by Barraclough et al. [4].

The conclusion is that the electronic configuration needs to be different, or direct exchange is more intense in the  $\text{FePc}$  form than in the  $\text{MnPc}$  form. It can be argued that the orbital ground state  $A_{2g} A_1 (d_{xy})^2 (d_{xz})^1 (d_{yz})^1 (d_{z^2})^1$ , proposed by Stillman et al. [24] leads to just antiferromagnetic coupling. The remaining configuration  $E_g B_1 (d_{z^2})^2 (d_{xz})^2 (d_{yz})^1 (d_{xy})^1$ , proposed by Labarta [15], generates a path for ferromagnetism in the  $\text{FePc}$  form: the unpaired electron in the  $d_{xy}$  orbital singlet may interact with its counterpart in the adjacent molecule via the  $E_g$

electron of the aromatic ring, which is orthogonal, giving rise to its ferromagnetic character (Fig. 12). This is the only ferromagnetic exchange path possible, however its intensity would be probably very weak since it is in the  $xy$  plane and the overlap will be small. At any rate, in the  $\text{FePc}$  form the  $d_{xy}$  orbital has negligible overlap with the  $E_g$  electron of the apical N since it is located in the  $z$  axis, thus the ferromagnetic interaction would be negligible. The unpaired electron of the  $(d_{xz}; d_{yz})$  doublet would lead in both forms to antiferromagnetic interaction. So, exchange interaction is not likely to cause the ferromagnetic coupling present in the  $\text{FePc}$  form.

On the other hand the condition for an enhancement with respect to the  $\text{FePc}$  form of the direct Fe-Fe interaction are fulfilled since the Fe-Fe distance is reduced from 4.8 Å to 3.8 Å. Following Goodenough [25], the direct ferromagnetic interaction occurs when there is overlap between a half-filled and an empty orbital, or a half-filled and a full orbital. Since the  $(d_{xz}; d_{yz})$  empty orbital is very high in energy [15] we think that only the case of half-filled full-orbital overlap may be relevant here. Then, if the orbital configuration is  $E_g A_1 (d_{xy})^2 (d_{xz})^2 (d_{yz})^1 (d_{z^2})^1$ , as proposed by Coops et al. for the  $\text{FePc}$  form from accurate X-ray diffraction [23], the overlap may take place between two  $(d_{xz})^2 (d_{yz})^1$  orbitals. The proposition of the  $E_g A_1$  electronic configuration by these authors is based on very direct observation of electronic deformation densities and in turn supports the proposed mechanism for the ferromagnetism in the  $\text{FePc}$  form. Of course, this overlap will decay strongly when the atoms are separated further by 1 Å, and so the ferromagnetic interaction weakens to the extent of being negligible in the  $\text{FePc}$  form.

Thus, we conclude that the difference in the phenomenology of the Mn and Fe forms can be related to the different ground state spin configuration (two magnetic doublets for Mn, and one magnetic doublet and a non-magnetic singlet for Fe) on the one hand, and to the different electron filling scheme and overlap probabilities of the resulting orbitals, on the other.

As said in the introduction, such a different behavior, ferromagnetism or paramagnetism, between two herringbone structured compounds formed by stacked square planar molecules containing Fe, has also been detected in Fe(II) octaethyltetraazaporphyrin [6, 7]. Similarly, the  $\text{FePc}$  form is ferromagnetic while the  $\text{MnPc}$  form is paramagnetic. However, in a recent paper [26] a magnetic study

of Mn(II) octaethyltetraazaporphyrin shows that the  $\beta$ -form is also ferromagnetic while the  $\alpha$ -form is paramagnetic, in contrast to the behavior of the MnPc form. So, the parallelism between the phthalocyanines and octaethyltetraazaporphyrin is not complete.

On the basis of the above, it appears to be beyond doubt that the magnetic moment of the Fe(II) in the  $\beta$ -FePc is to be associated with a spin triplet probably split by crystal field into a doublet and a lower-lying singlet. We then have to reconcile this conclusion with the rather low values of the magnetization reached even in high fields as exemplified in Figs. 8 & 10. Based on an effective spin  $S = 1$  and the powder  $g$ -value of 2.54 deduced from the Curie-Weiss fit to the susceptibility above 50 K, the saturation moment should amount to  $2.5 \mu_B$  per ion, i.e. far above the measured value even for an applied field of 200 kOe. Looking more closely at the measured  $M(H)$  curves and neglecting for the moment the relaxation effects, one may observe that below about 10 K the magnetization process can be divided in two steps. From the  $M(H)$  curve measured at 5 K (Fig. 8), a very rapid increase of the magnetization up to  $1.0 \mu_B$  (per atom) is observed for fields up to 400 Oe, followed by a much slower gradual increase up to the highest field applied. This two-step behavior can be explained in terms of a division of the magnetic chains into two different magnetic sublattices, with a mutually canted arrangement. In that case the fast rapid increase would correspond to saturation of the moments within each of the magnetic sublattices, followed by the gradual rotation of the sublattices to a common alignment parallel to the field. In the latter process, the Zeeman energy has to compete with the (large) crystal field anisotropy energy, so that the high-field susceptibility (slope of the  $M(H)$ ) curve can be very small. It is of interest to point out in this regard that for  $\beta$ -MnPc a canted magnetic structure in the above sense has indeed been reported [27].

At first sight the proposition that the ordered magnetic structure is canted seems to contradict the positive value of  $D$ , which implies a single crystal anisotropy of planar character. Indeed, Miyoshi et al. [27] concluded that for chains consisting of ferromagnetic coupled Fe moments with isotropic exchange, and with single-ion anisotropy, such that the quantization axis of the Fe sites in one chain is tilted by an angle which is opposite respect to the tilt angle in the adjacent chain, a negative  $D$  is needed to stabilize a canted structure, irrespectively if the interchain interaction is ferro or antiferromagnetic. This prediction, when applied to the MnPc compound, revealed a contradiction between the canted structure found in that compound by magnetization measurements and polarized neutron diffraction [3], and the positive  $D$  determined earlier from the analysis of the high-temperature susceptibility [28], a discrepancy that has gone unexplained so far. This apparently identical contradiction, now found for  $\beta$ -FePc and  $\beta$ -MnPc, can be explained by noting that, contrary to the assumption of Miyoshi et al. [27] that the ferromagnetic intrachain interaction

is isotropic, we find from our experiments that it is instead of the anisotropic Ising-type, with the easy axis perpendicular to the molecule plane. Interestingly, the same result; i.e. Ising intrachain interaction, was found to fit best the MnPc high temperature susceptibility by Barracough et al. [28], although it was not exploited. Thus, the Ising character of the interaction and its larger strength, comparable to the crystal field term, creates an uniaxial exchange anisotropy that opposes the crystal field anisotropy. A rough mean field calculation for FePc, using the value  $J = k_B \cdot 15$  K found from the Curie-Weiss fit, tells us that  $H_{ex} = (2zJ = k_B) \hbar S_z i = g \mu_B = 58$  T (at  $T = 0$  K). Such an intense field splits the upper  $S_z = 1$  doublet and brings the  $S_z = 1$  level 30 K down so that it nearly coincides with the  $S_z = 0$  level. The net effect is that, in terms of the  $S = 1$  formalism, the magnetic moment is polarized towards the quantization direction (local  $z$  axis) at low temperatures, which is the necessary condition to have the canted structure according to Miyoshi et al. [27]. In MnPc the exchange field is  $H_{ex} = 48$  T ( $D = k_B = 29$  K), and as a consequence the  $S_z = 3/2$  state is pulled below the  $S_z = 1/2$  state by 68 K (at  $T = 0$  K) and the ground state gives rise to an effective uniaxial anisotropy. Thus the annoying contradiction of an apparent inversion of the  $S_z = 3/2$  and  $S_z = 1/2$  states above and below the transition, mentioned at the end of Ref. [3], is resolved. In the paper by Rei et al. [26] on Fe-porphyrine, a similar qualitative argument of opposing exchange and crystal field effects is mentioned to explain the magnetic properties of those compounds.

The logical conclusion from the model we propose is that each chain has its own ferromagnetic axis tilted from the  $b$ -axis by a given angle, with the easy axis in the adjacent chain tilted by the opposite angle, for reasons of symmetry. Thus, in a domain formed by this ordered magnetic structure there is a direction of uncompensated moments, and a perpendicular direction of compensated moments. The uncompensated moments should have the direction of the  $b$ -axis in case the interchain interaction is ferromagnetic, and perpendicular to  $b$  if it is antiferromagnetic. In either cases, there are two degenerate types of domains, in contrast to the four of MnPc, due to the different symmetry. We refrain from pushing any further the analysis since we have insufficient experimental information on the magnitude and sign of the interchain interaction nor on the precise tilt angle, because our measurements are performed on powder samples.

We remark that the above analysis points to two different scenarios for analyzing the magnetic susceptibility data below 50 K, namely in terms of ferromagnetic Ising chains with either effective spin  $S = 1$ , or effective spin  $S = 1/2$ , when considering only the lowest two levels ( $S_z = 0$  and  $S_z = 1$ ). Below we shall investigate the applicability of both these possibilities.

Starting with  $S = 1$ , we have calculated the parallel susceptibility of an  $S = 1$  linear chain under the assumption of an Ising-like exchange interaction and of an uni-

axial single-ion anisotropy  $D$  as described by the Hamiltonian:

$$H_0 = -2J_1 \sum_{i=1}^N S_{z,i} S_{z,i+1} + D \sum_{i=1}^N S_{z,i}^2 - g_B \mu_B H_z \sum_{i=1}^N S_{z,i};$$

The eigenvalues  $\lambda_j$  of this Hamiltonian were obtained by the conventional transfer matrix technique, similarly as described in Ref. [29], yielding:

$$\lambda_0 = \frac{1}{2} (1 + \sqrt{1 + 4D}) \quad \lambda_1 = \frac{1}{2} [(1 + \sqrt{1 + 4D})^2 + 8J_1^2]^{1/2} \quad (5.1)$$

where  $\lambda_j = \exp[(2J_1 - D)/k_B T]$ ,  $\lambda_1 = \exp[(2J_1 + D)/k_B T]$  and  $\lambda_2 = \exp(D/2k_B T)$ , with  $\lambda_0$  being the largest eigenvalue. Utilizing a Taylor series expansion to obtain the eigenvalues in the non-zero-field case, the susceptibility can be expressed as

$$\chi = \frac{N g^2 \mu_B^2 S(S+1)}{k_B T} \frac{e^{2d} (e^j + 1 + e^j)}{F} \quad (5.2)$$

where

$$F = 3 + 2 + (1 + 2e^{j+2d}) [2e^{2d} (1 - e^j) - 2e^{4d} \sinh(2j)]; \quad (5.3)$$

with  $j = 2J_1/k_B T$  and  $d = D/2k_B T$ .

Least squares fits of Eq. (5.2) to the experimental susceptibility data were carried out. Since the contribution of the perpendicular susceptibility has been neglected, only the data for relatively high temperatures ( $T > 10$  K) were used. The dotted line in Fig. 4 shows the best fit with  $J_1/k_B = 25.7$  K,  $g = 2.54$  and  $D/k_B = 53.2$  K, where the positive  $J_1$  indicates ferromagnetic interaction and the positive  $D$  implies that the  $S_z = 1$  doublet lies above the  $S_z = 0$  state. The results are sensitive to both the temperature range utilized and the  $g$  value assumed. We have tried to fit the same data with the isotropic  $S = 1$  Heisenberg model and uniaxial anisotropy [30], but the fit is much worse (Fig. 4). For the temperature range from 20 to 300 K, the following result was obtained:  $J_1/k_B = 16.2$  K and  $D/k_B = 76.7$  K. Since we are fitting powder data while the magnetic properties are very probably highly anisotropic, the values obtained from the fit have to be considered as approximate. However, we note that the anisotropy constant is about half the value of  $D/k_B = 98$  K found in the  $\alpha$ -form [12]. Obviously, the different anisotropy originates from the absence of the apical N atoms next nearest to the Fe in the  $\beta$ -form respect to the  $\alpha$ -form. The most important result, though, is that the Fe(Fe intrachain interaction is unambiguously ferromagnetic. The value obtained for  $J_1$  is in fact similar to that following from the Curie-Weiss  $t$ .

We next turn to an analysis of the paramagnetic susceptibility below 50 K in terms of the effective spin  $S = 1/2$  formalism (Fig. 4), which would apply when

either the action of a crystal field of orthorhombic or lower symmetry, or the combined action of crystal field and magnetic exchange, would produce an effective doublet as the only occupied energy levels at low temperatures. In that case, since the effective anisotropy for the doublet will be of the Ising-type, we may compare the experimental powder susceptibility data with the theoretical predictions for the parallel ( $\chi_k$ ) and perpendicular ( $\chi_\perp$ ) susceptibilities for the ferromagnetic  $S = 1/2$  Ising chain [31]:

$$\chi_k = (N g_k^2 \mu_B^2 / 2J_{1/2}) K \exp(2K) \quad (5.4)$$

$$\chi_\perp = (N g_\perp^2 \mu_B^2 / J_{1/2}) [\tanh(K) + K \cosh^2(K)] \quad (5.5)$$

where  $K = J_{1/2}/2k_B T$ , from which we have calculated the powder susceptibility  $\chi_p = (\chi_k + 2\chi_\perp)/3$ . We can consider also that due to the large expected anisotropy one has  $g_k \gg g_\perp$ , and that the saturation magnetization at low temperature is  $M_p = \frac{1}{3}(g_k + 2g_\perp) S \mu_B$ , for which the experiment yielded  $1.5 \mu_B$ . Fitting both quantities (for  $T > 10$  K) leads to the estimates  $J_{1/2}/k_B = 32.2$  K,  $g_k = 8.6$  and  $g_\perp = 0.2$ . The fit of the magnetic susceptibility data with the prediction from the above equations is shown in Fig. 4. It is difficult to judge whether the fit on the basis of the  $S = 1$  model is better than that with the  $S = 1/2$  prediction since: (a) the deviations seen for  $T < 10$  K from the  $S = 1/2$  curve may well be due to the interchain interactions, which are not taken into account; (b) for the same reason the seemingly better fit with the  $S = 1$  model (Fig. 4) may be fortuitous since it also neglects interchain interactions; (c) as a further complication the  $\chi_\perp$  contribution had to be neglected in the  $S = 1$  calculation since no theoretical prediction is available.

Proceeding next to a discussion of the ordering/blocking phenomena observed below 10 K, we can start from the assertion that we may describe  $\beta$ -FePc as a system of very weakly coupled ferromagnetic Ising chains with either effective spin  $1/2$  or  $1$ . For such systems, it is well-known that the 1D magnetic behavior is dictated by the excitation of domain-walls (solitons) along the chains. For strongly anisotropic chains, the width of the domain-wall becomes smaller than a lattice constant and we speak of "kinks" separating spin-up and spin-down regions. At least two types of excitations in such Ising chains are possible. Namely, the single-kink excitations at the ends of the chains (with excitation energy  $J$ ) and the kink-pair excitations (with energy  $2J$ ). The correlation length along the chain (and thus the magnitude of the magnetic susceptibility) is determined by the number  $n_k$  of kinks excited ( $1/n_k \propto \exp(-J/k_B T)$ ).

Thus we think the present system falls in the same class of Ising-type chains studied previously, a.o. by magnetic susceptibility and Mossbauer effect studies, in connection with the soliton problem (see e.g. Refs. [32, 33, 34, 35, 36, 37, 38, 39]). In fact, the behavior observed here appears to be analogous to that of  $\text{FeCl}_2\text{Py}_2$ , one of the ferromagnetic Ising chains studied in these previous works.

However, for  $\text{-FePc}$ , the interchain coupling turns out to be much weaker than in  $\text{FeCl}_2\text{Py}_2$  and related compounds.

As already mentioned when presenting the Mossbauer data in Fig. 11, the extremely strong broadening of the spectra observed in the range 5 K { 20 K may indeed be explained in terms of a spin dynamics based upon the excitation of domain-walls along the ferromagnetic chains. Since the Mossbauer effect is sensitive to high-frequency fluctuations, the relaxation effects already start to have an influence at about 20 K, whereas relaxation effects in the low-frequency susceptibility appear only below 10 K. In principle, both the high- and low-frequency spin dynamics observed can be related to a gradual slowing down of the spin fluctuations with temperature due to the decrease of the density and the mobility of the walls, followed by (almost) complete pinning below 5 K. It should be realized that, even when pinned, small excursions around equilibrium positions of the walls may still remain possible, which explains the possibility of simultaneous observation of both the high- and low-frequency spin dynamics in the range between 10 K and 5 K.

At this point it is important to recall the similarity of the here-observed relaxation phenomena with those known for superparamagnetic particles pointed out several times in the above. Indeed, one might envisage the ferromagnetic chains in  $\text{-FePc}$  as superparamagnetic particles, switching their magnetization among the up and down directions along the local anisotropy axis. However, it should then be immediately realized that the rotation of the spins along a given chain cannot occur simultaneously, in view of the extremely large anisotropy barrier involved in such a process (i.e. the anisotropy per spin times the number of spins in a correlated chain). In full analogy with the situation in ferromagnetic nanowires [40], the rotation has to occur via the excitation of a small reversed domain, either at the chain end by a  $\pi$ -wall, or along the chain by a kink-antikink pair, in both cases followed by the propagation along the chain of the wall(s). It is clear then, that the mobility of the domain-wall(s) along the chains may become an important factor in determining the speed of the switching process. In this respect the magnetic interactions between the chains, which tend to establish full 3D order between correlated chain segments as the temperature is lowered, can be expected to slow down the wall motions along the individual chains. It is tempting, therefore, to associate the slowing down of the fluctuations in the range between 10 K and 5 K, seen in both the Mossbauer spectra and the ac-susceptibility, as a reflection of the gradual establishment of 3D magnetic order between the chains. Since no clear transition at a definite temperature  $T_C$  is indicated, the resulting "order" is apparently not long-range but with a substantial amount of randomness, as in a spin glass. Judging from the behavior seen in e.g. Figs. 6 and 7 of the low-field magnetization, this ordering process is about completed below 5 K. The source of randomness is probably a ran-

dom pinning of the domain-walls on impurities along the chain, whereby the 3D magnetic correlations between the chains are easily broken up. In view of the instability of  $\text{-FePc}$  in favor of the  $\text{-FePc}$  form, the occurrence of such impurities is not unlikely.

The above scenario can also explain the fact that in our specific heat data measured in the range 1.8 K to 20 K, no sign of a singularity (as associated with 3D long-range magnetic ordering) was detected. The measured specific heat curve just shows a smooth continuous behavior as expected for a combination of phonon contributions and 1D magnetic fluctuations within the chains.

Adopting therefore tentatively the value of 5 K as representative temperature for the ordering process between the chains, we may estimate the interchain coupling  $J^0$  either from the Oguchi's formula [41], or from the mean-field argument given by Villain [42], in both cases obtaining  $J^0 = k_B (10^3 - 10^2)$  K. This estimate may be confronted with the behavior of the magnetization curves taken at 5 K and 8 K (Fig. 8), in which as discussed before a rapid initial "saturation" mechanism is observed at an applied field of 400 Oe only. In the canting mechanism discussed above, we have ascribed this low-field process with an alignment of all the spins on the individual sublattices. This implies the removal by the field of all domain-walls along the chains, as well as the breaking up of the interchain interactions. It follows that the effective field  $H^0 = z^0 J^0 S / g \mu_B$  should be smaller than 400 Oe, which yields (taking  $g \approx 2$ , and  $S = 1$ ) the upper limit  $J^0 = k_B < 0.03$  K. This would suggest in fact that the breaking up of the interchain couplings occurs in even much smaller fields already and that the magnetization process up to 400 Oe mainly involves the removal of the domain-walls from the chains by the Zeeman energy.

The quite peculiar form of the hysteresis in Fig. 10 appears to agree with the just sketched scenario. After first saturating the chain system, the ferromagnetic order within and between the chains is seen to remain intact until the applied field is reduced to effectively zero, whereafter the magnetization discontinuously drops to zero. The instability of the ferromagnetic order in zero-field even at 1.8 K indicates that the interchain interaction is most probably antiferromagnetic. As soon as the applied field has become smaller than this antiferromagnetic coupling, it will tend to order the ferromagnetic chains back again into an antiparallel arrangement. This means that half of the chains will have to switch their magnetization and as we have argued in the above, this can only occur by the excitation and subsequent propagation of domain-walls. Part of these walls will then become pinned again so that the antiferromagnetic arrangement can not become complete and when subsequent by increasing the field in the opposite direction, the same cycle of removal of the walls has to be overcome.



## VI. CONCLUDING REMARKS

Clearly at variance with all previously reported behavior of both polytypes of iron (II) phthalocyanine, we have found that the magnetic structure of  $\alpha$ -FePc can be described in terms of ferromagnetic Ising chains, with very weak antiferromagnetic interchain coupling. As a consequence of impurities and other possible lattice defects, the transition to 3D ordering is suppressed, so that instead, a gradual freezing/blocking transition is observed to a disordered magnetic state. The disorder is lifted by a small field of about 2 kOe. Below 5 K this transition is hindered by strong relaxation effects, which we attribute to the pinning of the domain-walls by the randomly distributed defects in combination with the interchain coupling. The competition between magnetic exchange interaction and crystal field effect gives rise to a canted arrangement of the ferromagnetically aligned spins. Above 10 K the behavior of the susceptibility can be interpreted in terms of the thermal excitation of kinks (domain-walls) and kink-antikink pairs. Preliminary Mossbauer experiments can be consistently explained in the same terms, the kink dynamics being re-

ected in the spectra in the form of strong relaxation effects. The excitation and dynamics of the kinks lead to line-broadening and hyperfine-splitting of the spectra at elevated temperature, i.e. far into the paramagnetic region.

## Acknowledgments

This paper is dedicated to Prof. Dr. Domingo Gonzalez Alvarez on the occasion of his retirement. We are indebted to F. Luis, F. Palacio and J. F. Fernandez for helpful discussions, M. C. Sanchez for the X-ray experiments in Zaragoza, J. A. A. J. Perenboom and H. van Luong for the high-field magnetization experiments at the FOM-IGM facility in Nijmegen, and M. Laguna for the chemical analysis in Zaragoza. The financial support inside of Spain (Romania Scientific Co-Operation program by the Ministerio de Asuntos Exteriores and the Agentia Nationala pentru Stiinta, Tehnologie si Inovare is gratefully acknowledged. This work was also partially supported by Grant No. MAT 99/1142 from CICYT.

- 
- [1] C. C. Lezno and A. B. P. Lever (Eds.), *Phthalocyanines: Properties and Applications*, (VCH Publishers, New York, 1996), Vol. 4.
  - [2] M. J. Cook, *J. Mater. Chem.* **6**, 677 (1996).
  - [3] S. Mitra, A. Gregson, W. Hatfield and R. Weller, *Inorg. Chem.* **22**, 1729 (1983).
  - [4] C. G. Barraclough, R. L. Martin, S. Mitra and R. C. Sherwood, *J. Chem. Phys.* **53**, 1643 (1970).
  - [5] B. Honigsmann, H. U. Lenne and R. Schroedel, *Z. Kristallogr., Kristallgeom., Kristallphys., Kristallchem.* **122**, 185 (1965).
  - [6] G. Yee, B. Korte, S. Sellers, W. Rei and Ch. Frommen, *Mol. Cryst. Liq. Cryst.* **335**, 23 (1999).
  - [7] S. P. Sellers, B. J. Korte, J. P. Fitzgerald, W. M. Rei and G. T. Yee, *J. Am. Chem. Soc.* **120**, 4662 (1998).
  - [8] S. E. Harrison and K. H. Ludewig, *J. Chem. Phys.* **45**, 343 (1966).
  - [9] C. Ercolani, C. Neri and P. Porta, *Inorg. Chim. Acta* **1**, 415 (1967).
  - [10] L. Klemm and W. Klemm, *J. Prakt. Chem.* **143**, 82 (1935).
  - [11] A. B. P. Lever, *J. Chem. Soc.*, 1821 (1965).
  - [12] B. W. Dale, R. J. Williams, C. E. Johnson and T. L. Thorp, *J. Chem. Phys.* **49**, 3441 (1968).
  - [13] D. Luneau, *Curr. Opin. Solid State Mat. Science* **5**, 123 (2001).
  - [14] P. D. W. Boyd, T. D. Smith, J. H. Price and J. R. Pilbrow, *J. Chem. Phys.* **56**, 1253 (1972).
  - [15] A. Labarta, E. Molins, X. Vinas, J. Tejada, A. Caubet and S. Alvarez, *J. Chem. Phys.* **80**, 444 (1984).
  - [16] L. J. de Jongh and A. R. Miedema, *Adv. Phys.* **50**, 947 (2001), (Reprinted from *Adv. Phys.* **23**, 1974).
  - [17] J. J. M. Steijger, E. Frikkee, L. J. de Jongh and W. J. Huiskamp, *Physica* **123B**, 271 (1984).
  - [18] J. A. Mydosh, *Spin Glasses: An Experimental Introduction* (Taylor and Francis LTD., London, 1993).
  - [19] A. Abragam and B. Bleaney, *Electron Paramagnetic Resonance of Transition Ions*, (Oxford University Press, London, 1970), p. 153.
  - [20] J. T. Schriepf and S. A. Friedberg, *Phys. Rev.* **136**, A 518 (1964).
  - [21] T. Moriya, *Phys. Rev.* **177**, 635 (1960).
  - [22] H. Yamada, T. Shimada and A. Komatsu, *J. Chem. Phys.* **108**, 10256 (1998).
  - [23] Ph. Coppens, L. Li and N. J. Zhu, *J. Am. Chem. Soc.* **105**, 6174 (1983).
  - [24] M. J. Stillman and A. J. Thompson, *J. Chem. Soc. Far. II* **70**, 790 (1974).
  - [25] J. B. Goodenough, in *Magnetism and the Chemical Bond*, Interscience Chem. Sec., F. A. Cotton (Ed.), (John Wiley & Sons, New York, 1966), Vol. 1, pag. 166.
  - [26] W. M. Rei, C. M. Frommen, G. T. Yee and S. P. Sellers, *Inorg. Chem.* **39**, 2076 (2000).
  - [27] H. Miyoshi, *J. Phys. Soc. Japan* **37**, 1950 (1974).
  - [28] C. G. Barraclough, A. K. Gregson and S. Mitra, *J. Chem. Phys.* **60**, 962 (1974).
  - [29] S. O'Brien, R. M. Gaura, C. P. Landee and R. D. W. Illett, *Solid State Commun.* **39**, 1333 (1981).
  - [30] T. De Neef, Ph.D. Thesis, Eindhoven (1975).
  - [31] S. Katsura, *Phys. Rev.* **127**, 1508 (1962).
  - [32] R. C. Thiel, H. de Graaf and L. J. de Jongh, *Phys. Rev. Lett.* **47**, 1415 (1981).
  - [33] L. J. de Jongh, C. A. M. Mulder, R. M. Comelisse, A. J. van Duyneveldt and J. P. Renard, *Phys. Rev. Lett.* **47**, 1672 (1981).
  - [34] L. J. de Jongh, *J. Appl. Phys.* **53**, 8018 (1982).
  - [35] H. J. M. de Groot, L. J. de Jongh, R. C. Thiel and J. Reedijk, *Phys. Rev. B* **30**, 4041 (1984).

- [36] H . H . A . S m i t , H . J . M . de G root , R . C . Thiel , L . J . de Jongh , C . E . Johnson and M . F . Thom as , Solid State Commun . 53 , 573 (1985) .
- [37] H . H . A . S m i t , H . J . M . de G root , M . E M assalam i , R . C . Thiel and L . J . de Jongh , Physica B 154 , 237 (1989) .
- [38] M . E M assalam i and L . J . de Jongh , Physica B 154 , 254 (1989) .
- [39] M . E M assalam i , H . H . A . S m i t , R . C . Thiel and L . J . de Jongh , Physica B 154 , 267 (1989) .
- [40] H . B . Braun , J . Appl Phys . 85 , 6172 (1999) .
- [41] T . O guchi , Phys . Rev . B 113 , A 1098 (1964) .
- [42] J . Villain and J . M . Loveluck , J . Phys . Lett . 38 , L77 (1977) .

## LIST OF FIGURES

1. Images of powder  $\text{-FePc}$ .
2. Molecular structure of  $\text{FePc}$  and its stacking along the b-axis.
3. Inverse of the in-phase zero-field susceptibility as a function of temperature for an exciting field with frequency  $f = 90 \text{ Hz}$ . In the inset: the same data but as  $\chi''$  versus  $T$ . The susceptibility of  $\text{-FePc}$  is reported for comparison. The solid curve is the fit to the Curie-Weiss law  $\chi = C/(T - \theta)$ , where  $C = g^2 \mu_B^2 S(S + 1)/4k_B$ .
4. In-phase zero-field susceptibility as a function of temperature for an exciting field with frequency  $f = 90 \text{ Hz}$ . The lines are the calculated susceptibilities in terms of the effective spin  $S = 1$  (above) and  $S = 1/2$  (below). For explanations see text.
5. Low-temperature in-phase and out-of-phase susceptibilities for several frequencies.
6. Molar magnetization vs temperature measured during heating after ZFC (5) and FC (4) in an applied field  $H_{\text{ap}} = 50 \text{ Oe}$  and  $H_{\text{ap}} = 1 \text{ kOe}$ .
7. Remanence of the magnetization after a FC process with  $H = 40 \text{ Oe}$ . In the inset: magnification of the "lower slope" region.
8. Molar magnetization vs applied field recorded by increasing the field and at different temperatures:  $T = 1.8 \text{ K}, 5 \text{ K}, 8 \text{ K}, 15 \text{ K}$  and  $30 \text{ K}$ . The measuring time is  $150 \text{ s}$ . In the inset: magnification of the magnetization recorded at  $5 \text{ K}$  for low-field values.
9. High field molar magnetization recorded at  $T = 5 \text{ K}$  varying the field from null to  $200 \text{ kOe}$  and to null again with a measuring time of  $40 \text{ s}$ . For comparison, the data from Fig. 8 are depicted (filled symbols).
10. Hysteresis loop recorded at  $T = 1.8 \text{ K}$ . A field of  $50 \text{ kOe}$  is first applied and then data are collected by sweeping the field to  $50 \text{ kOe}$  and back.
11. Representative Mossbauer spectra taken at different temperatures. Above  $25 \text{ K}$ , the shape of the spectra is almost independent of temperature.
12. A schematic of  $a_g\{E_g\}$  interaction for  $\text{-form}$  (a) and  $\text{-form}$  (b), and  $e_g\{E_g\}$  interaction for  $\text{-form}$  (c) and  $\text{-form}$  (d).

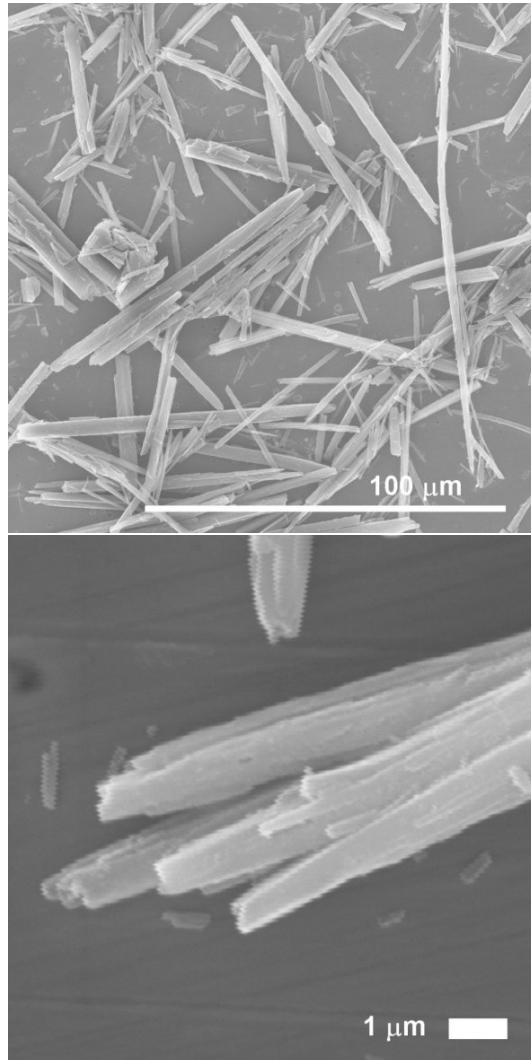


Fig. 1, M. Evangelisti et al., PRB

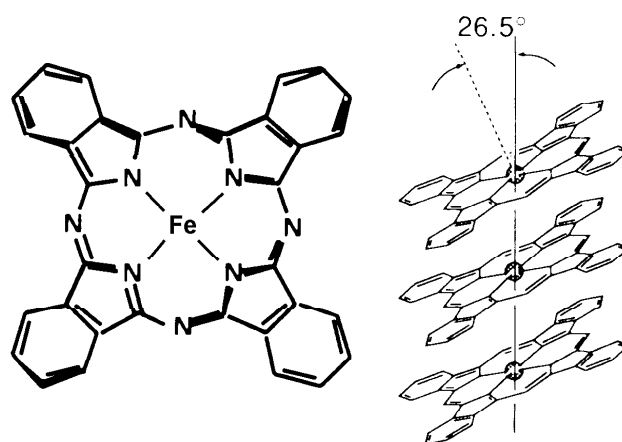


Fig. 2, M. Evangelisti et al., PRB

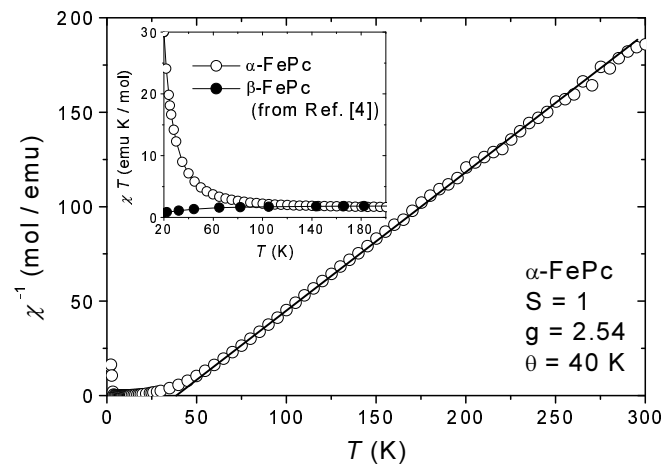


Fig. 3, M. Evangelisti et al., PRB

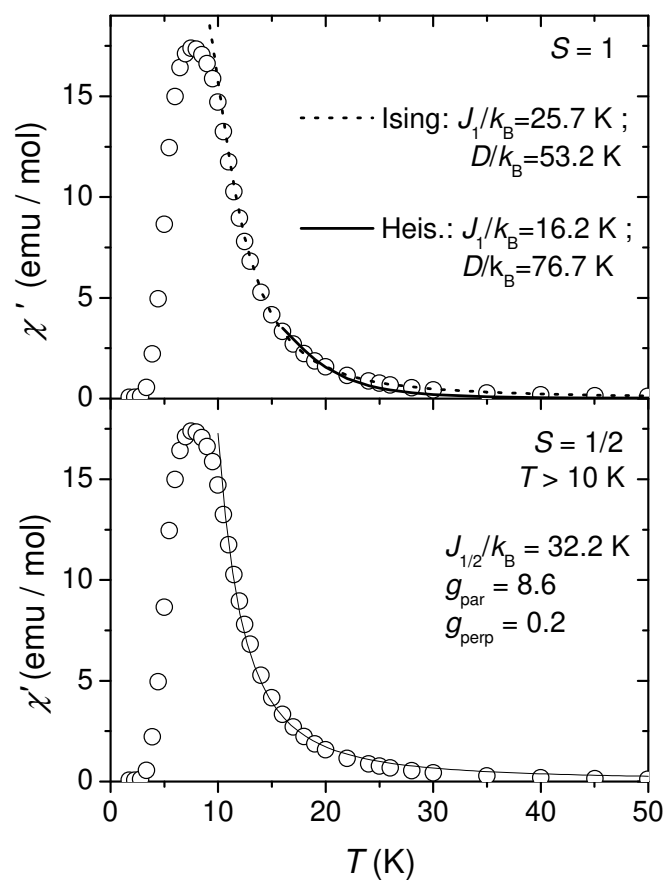


Fig. 4, M. Evangelisti et al., PRB

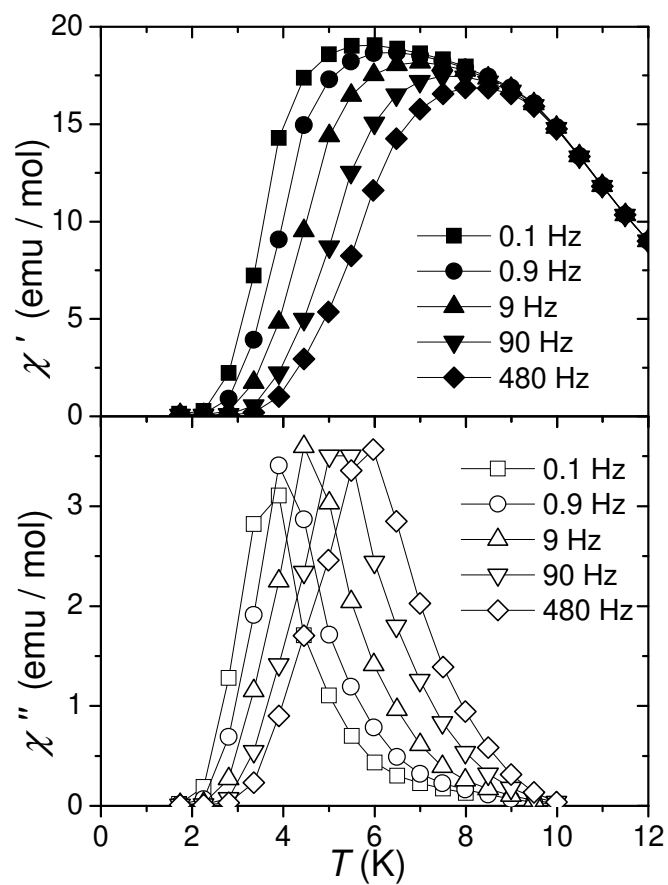


Fig. 5, M. Evangelisti et al., PRB



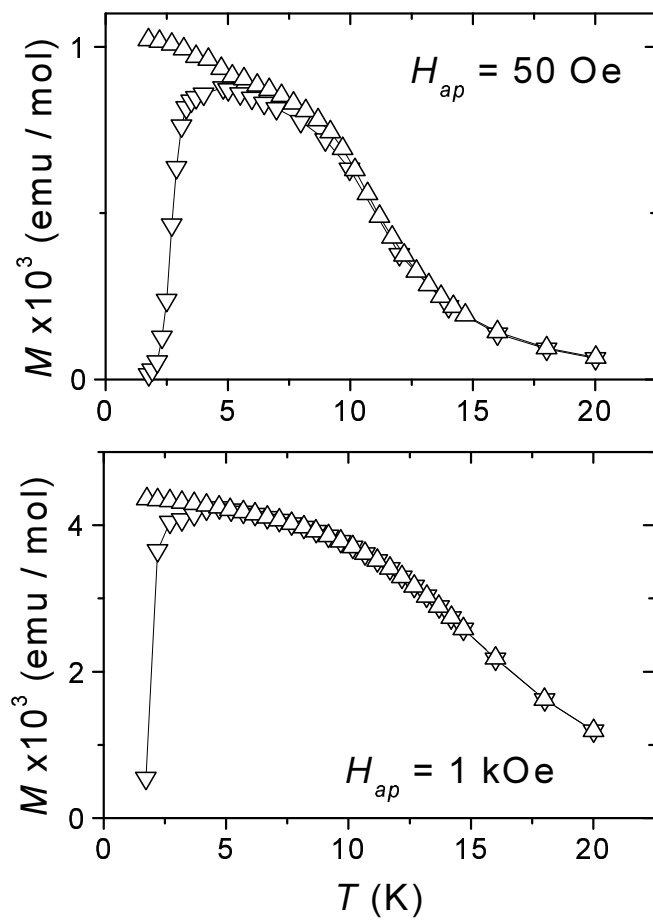


Fig. 6, M. Evangelisti et al., PRB

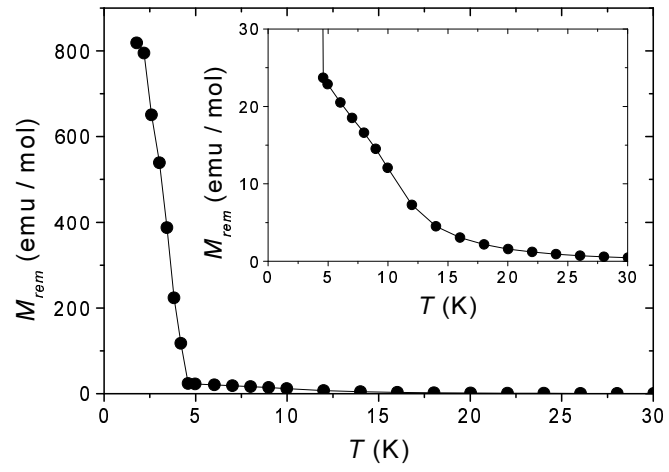


Fig. 7, M. Evangelisti et al., PRB

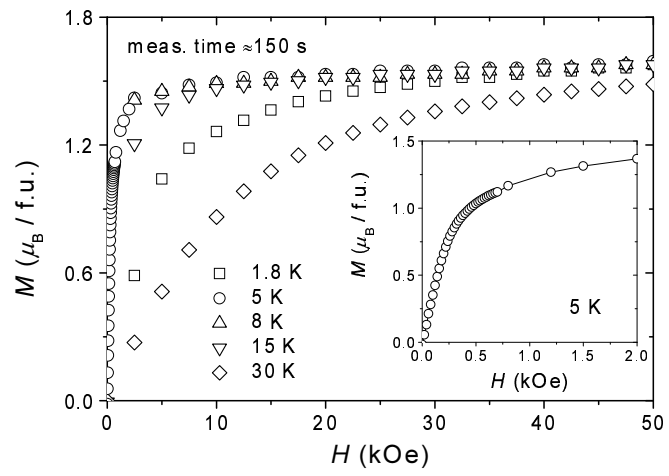


Fig. 8, M. Evangelisti et al., PRB

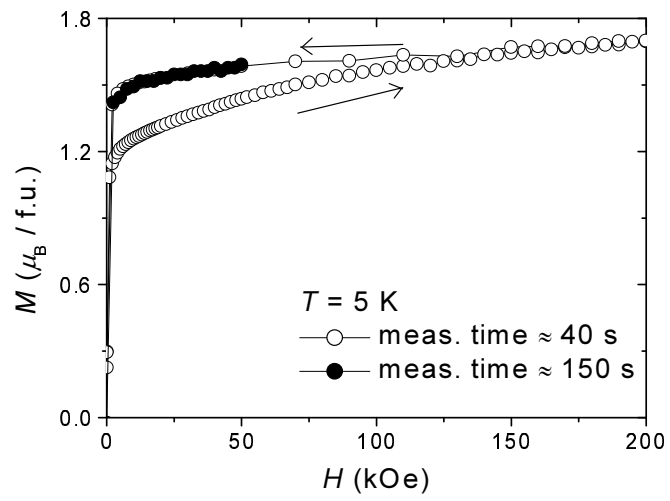


Fig. 9, M. Evangelisti et al., PRB

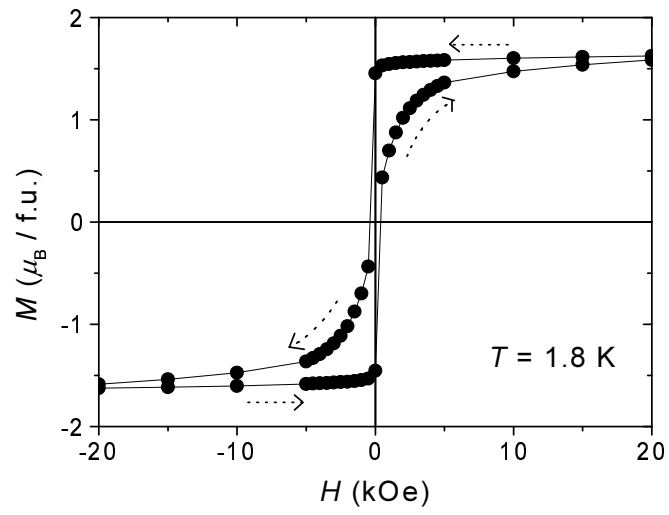


Fig. 10, M. Evangelisti et al., PRB

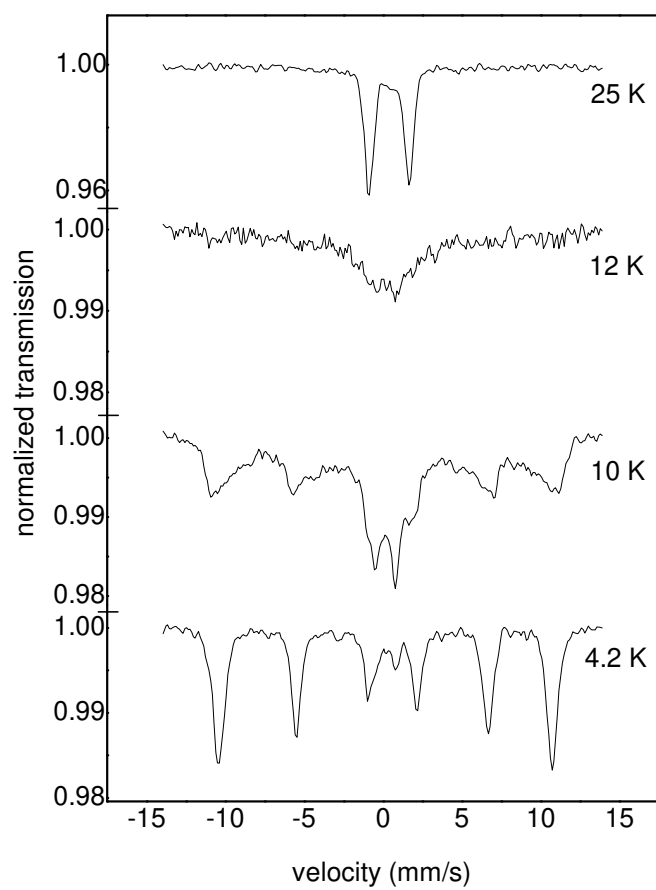


Fig. 11, M. Evangelisti et al., PRB

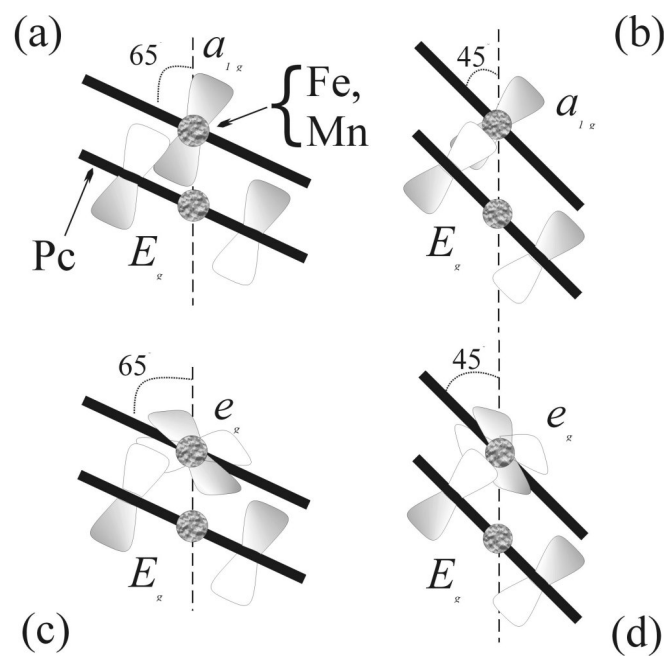


Fig. 12, M. Evangelisti et al., PRB